

Bromodomain-containing protein 4 is critical for the antiproliferative and pro-apoptotic effects of gambogic acid in anaplastic thyroid cancer

YONGHUI WANG¹, WEI WANG² and HONGQIN SUN³

¹Department of Breast Surgery, Weifang People's Hospital, Weifang, Shandong 261041;

²Department of Breast, Thyroid and Hernia Surgery, Liaocheng People's Hospital, Liaocheng, Shandong 252000;

³Department of Central Sterile Supply, Weifang People's Hospital, Weifang, Shandong 261041, P.R. China

Received October 31, 2017; Accepted April 19, 2018

DOI: 10.3892/ijmm.2018.3642

Abstract. Gambogic acid (GA) has been widely used as an anticancer drug for different tumors, including thyroid cancer. However, the potential function and molecular mechanisms of GA in anaplastic thyroid cancer (ATC) has not been illustrated thus far. The aim of the present study was to demonstrate the antitumor effects of GA on ATC cells and investigate its underlying molecular mechanisms. The results revealed that GA significantly decreased the viability and proliferation, as well as induced cell apoptosis in ATC cell lines. Next, it was demonstrated that GA decreased the expression of bromodomain-containing protein 4 (BRD4), which has been reported to function as an oncogene in various types of cancer. BRD4 expression was significantly higher in ATC tissues compared with that in adjacent normal thyroid tissues. In addition, BRD4 silencing significantly repressed the cell viability and proliferation, and increased the cell apoptotic rate *in vitro*, while it also delayed the tumor growth *in vivo*. Notably, ectopic BRD4 expression significantly weakened the biological effects of GA on ATC cells *in vitro* and *in vivo*, which suggested that GA served its anticancer functions partially via downregulating BRD4. In conclusion, BRD4, functioning as an oncogene in ATC, is important for the antiproliferative and pro-apoptotic effects of GA.

Introduction

Thyroid cancer incidence is rapidly increasing in the USA, and its estimated annual diagnosis and mortality rates in 2017 were 56,870 and 2,010 cases, respectively. Thyroid cancer is typically

classified as papillary, follicular and anaplastic carcinoma (1). Amongst these classifications, anaplastic thyroid cancer (ATC) accounts for 1-2% of all thyroid tumors. ATC is characterized by aggressive and local invasion, and common distant metastasis (2). Currently, the available therapies for ATC include chemotherapy, radiotherapy and surgery; however, effective targeted treatments have yet to be developed. ATC remains one of the most fatal types of cancer, with a mean survival time of 6 months (3). Therefore, an enhanced understanding of the molecular mechanisms underlying the carcinogenesis and progression of ATC would contribute to the development of novel diagnostic markers and therapeutic targets.

Gambogic acid (GA), the main active ingredient of gamboge, is a brownish orange dry resin secreted from the plant *Garcinia hanburyi* that is widely distributed in nature. GA has been reported to inhibit the growth of different types of cancer, including lung, colorectal, prostate and breast cancer, hepatocellular carcinoma, multiple myeloma and leukemia (4-10). The possible mechanisms underlying the antitumor effect of GA are associated with the induction of apoptosis, inhibition of telomerase, interruption of nuclear factor- κ B signaling pathway and enhancement of reactive oxygen species accumulation (5,9,11). However, the potential effect and underlying molecular mechanisms of GA in ATC remain poorly understood.

Bromodomain-containing protein 4 (BRD4) is an epigenome reader and a member of the bromodomain and extra-terminal domain (BET) family of proteins, which are composed of two bromodomains in tandem and an extra-terminal domain. BRD4 has been reported to promote cell cycle progression and to regulate cell growth and transcription (12). Furthermore, it participates in tumor growth and proliferation in various tumors, including in lymphoblastic leukemia, glioblastoma, neuroblastoma, malignant peripheral nerve sheath tumors, melanoma, lung adenocarcinoma and papillary thyroid cancer (13-21). However, the role of BRD4 in ATC has yet to be described in detail.

In the present study, the antiproliferative effect of GA in ATC cells by inducing cell apoptosis was initially confirmed. In addition, it was demonstrated that BRD4 was a potential target of GA, and that BRD4 silencing suppressed tumor

Correspondence to: Dr Hongqin Sun, Department of Central Sterile Supply, Weifang People's Hospital, 151 Guangwen Street, Weifang, Shandong 261041, P.R. China
E-mail: sunhongqin001@sina.com

Key words: bromodomain-containing protein 4, gambogic acid, proliferation, apoptotic, anaplastic thyroid cancer

growth *in vitro* and *in vivo*. Furthermore, *in vitro* and *in vivo* experiments indicated the critical role of BRD4 in the antiproliferative effects of GA on ATC cells.

Materials and methods

Cell culture and tissue collection. The human normal thyroid Nthy-ori 3-1 cell line and two ATC cell lines (SW1736 and KAT-18) were obtained from the American Type Culture Collection (Manassas, VA, USA). The cell lines were authenticated using short-tandem repeat profiling performing by BMR Genomics (Padova, Italia). The cells were maintained in Dulbecco's modified Eagle's medium (HyClone; GE Healthcare Life Sciences, Beijing, China) with 10% fetal bovine serum (HyClone; GE Healthcare Life Sciences) in a humidified atmosphere with 5% CO₂ and 95% air at 37°C. For the Cell Counting Kit-8 (CCK-8) assay, SW1736 and KAT-18 cells were cultured with increasing doses of GA (Key Laboratory of Carcinogenesis and Intervention, China Pharmaceutical University, Nanjing, China; 0, 2, 4 and 6 µg/ml) for 48 h or treated with 2 µg/ml GA for the indicated time points (0, 24, 48 and 72 h) at 37°C. For the colony formation assay and flow cytometry, SW1736 and KAT-18 cells were cultured with increasing doses of GA (0, 2, 4 and 6 µg/ml) for 48 h at 37°C. To discover the association between BRD4 and GA, ATC cells were then divided into four groups, treated with BRD4 overexpression plasmid with dimethyl sulfoxide (DMSO), BRD4 overexpression plasmid with 2 µg/ml GA, control vector with DMSO, and control vector with 2 µg/ml GA.

Furthermore, human ATC specimens and their adjacent normal thyroid tissues (10 pairs) were collected from 10 patients (3 males and 7 females; age range, 51-70 years; median age, 62) who underwent surgery at the Weifang People's Hospital (Weifang, China) between January 2017 and October 2017. All ATC specimens were confirmed by pathological diagnosis according to the World Health Organization criteria (22). The present study was approved by the Ethics Committee of Weifang People's Hospital (Weifang, China). Written informed consent was obtained from each patient who participated in this study.

Cell transfection. shRNA plasmids for BRD4, which were designed against the BRD4 gene and constructed in Phblv-u6-puro vectors, were purchased from Hanbio Biotechnology Co., Ltd. (Shanghai, China). A non-target scrambled oligonucleotide functioned as the negative control. To generate stable BRD4 knockdown cells, SW1736 and KAT-18 cells were grown in six-well plates until they reached 40% confluence. The medium was replaced with 1 ml Dulbecco's modified Eagle's medium (HyClone; GE Healthcare Life Sciences, Beijing, China) supplemented with 100 µl viral supernatant (1x10⁸ UT/ml) and 8 µg/ml polybrene (Hanbio Biotechnology Co., Ltd.) for 24 h. The SW1736 and KAT-18 cells were further cultured in Dulbecco's modified Eagle's medium (HyClone; GE Healthcare Life Sciences, Beijing, China) with 10% fetal bovine serum (HyClone; GE Healthcare Life Sciences) containing puromycin (Hanbio Biotechnology Co., Ltd.) at 5 and 3 µg/ml at 37°C for three passages, respectively. Individual puromycin-resistant colonies were isolated

during drug screening. The shRNA sequences used in the present study were as follows: shBRD4, 5'-GatccGCCTGG AGATGACATAGTCTTATTCAAGAGATAAGACTATGT CATCTCCAGGTTTTTTC-3'; and shControl, 5'-GatccTTC TCCGAACGTGTACGTAATTCAAGAGATTACGTGAC ACGTTCCGAGAATTTTTTg-3'. A non-target scrambled oligonucleotide functioned as the negative control and presented no homology to any human transcripts. Furthermore, BRD4 overexpression was examined using BRD4 overexpression plasmid and control vectors that were obtained from Santa Cruz Biotechnology, Inc. (Dallas, TX, USA). Cell transfection was conducted according to the manufacturer's protocol.

Cell viability assay. Cell viability was examined using a CCK-8 assay. Briefly, SW1736 and KAT-18 cells were plated into a 96-well plate (3,000 cells/well). After 0, 24, 48 and 72 h of incubation, 10 µl CCK-8 solution (Beyotime Institute of Biotechnology, Haimen, China) was added into each well at 37°C. Following 3 h of culturing, the absorbance of each well was determined using a Multiskan MK3 device (Thermo Fisher Scientific, Inc., Waltham, MA, USA) at a wavelength of 450 nm.

Colony formation assay. SW1736 and KAT-18 cells were cultured in a 6-well plate at a density of 300 cells/well. After 7 days, the cells were washed with phosphate-buffered saline (PBS), fixed with paraformaldehyde and stained with crystal violet. Subsequently, the number of the colonies that had migrated through the pores was quantified by randomly counting 10 independent visual fields using the images.

Cell apoptosis analysis. Cell apoptosis was assessed using flow cytometry with staining of the cells using an Annexin V/propidium iodide (PI) kit (Nanjing KeyGen Biotech Co, Ltd., Nanjing, China) according to the manufacturer's protocol. Briefly, cells seeded in 24-well plates were exposed to 0, 2, 4 and 6 µg/ml of GA for 48 h, then cells were collected and washed twice in ice cold PBS. The washed cells (2x10⁵/well) were resuspended in 100 µl binding buffer (included in the kit) and stained with 5 µl Annexin V and 5 µl PI for 15 min at room temperature. Following incubation for 15 min in the dark at room temperature, flow cytometry was performed. A flow cytometer (Cytomics FC 500 MPL; Beckman Coulter, Inc., Brea, CA, USA) was utilized to evaluate the apoptotic levels in each sample according to the manufacturer's protocol. Data were analyzed using ModFit LT 3.0 (Verity Software House, Inc., Topsham, ME, USA).

Reverse transcription-quantitative polymerase chain reaction (RT-qPCR). Total RNA was extracted from tissues and cells by using TRIzol reagent (Invitrogen; Thermo Fisher Scientific, Inc.) according to the manufacturer's protocol. The concentration of total RNA was determined by spectrophotometry (TECAN Infinite® F200PRO microplate reader; Tecan Group, Ltd., Mannedorf, Switzerland). For mRNA expression analysis, RNA was reverse transcribed into cDNA using a PrimeScript RT reagent kit with gDNA Eraser (Takara Biotechnology Co., Ltd., Dalian, China). qPCR was then conducted using SYBR Premix Ex Taq (Takara Biotechnology Co., Ltd.). The qPCR

conditions were applied for detecting mRNAs: 95°C for 30 sec, followed by 40 cycles of 95°C for 30 sec, 60°C for 30 sec and 72°C for 30 sec using the following primers: BRD4 forward, 5'-CATGGACATGAGCACAATCA-3', and reverse, 5'-TCA TGGTCAGGAGGGTTGTA-3'; β -actin forward, 5'-GATCAT TGCTCCTCCTGAGC-3', and reverse, 5'-ACTCCTGCTTGC TGATCCAC-3'. β -actin served as the internal control. The specificity of amplification was examined using melting curve analysis and electrophoresis in 1% agarose gel. The relative expression level of the target gene mRNA was calculated as the inverse log of $\Delta\Delta C_q$ and normalized to the internal control (23).

Western blot analysis. SW1736 and KAT-18 cells were lysed to extract the total protein by using RIPA lysis buffer (Promega Corporation, Madison, WI, USA) according the manufacturer's instructions. Protein concentration was determined using a BCA Protein Assay kit (Thermo Fisher Scientific, Inc.) according the manufacturer's protocol. Next, the same amount of protein (40 μ g) from each cell line was subjected to 12% SDS-PAGE and transferred onto polyvinylidene difluoride membranes. The membranes were then respectively incubated with various diluted primary antibodies against BRD4 (1:200; cat. no. ab75898; Abcam, Cambridge, MA, USA), B-cell lymphoma 2 (Bcl-2; 1:500; cat. no. sc7382; Santa Cruz Biotechnology, Inc.), Bcl-2-associated X protein (Bax; 1:500; cat. no. sc7480; Santa Cruz Biotechnology, Inc.), cleaved caspase-3 (1:500; cat. no. #9661; Cell Signaling Technology, Inc., Beverly, MA, USA), cleaved poly(ADP-ribose) polymerase (PARP; 1:500; cat. no. #5625; Cell Signaling Technology, Inc.) or β -actin (1:800; cat. no. AA128; Beyotime Institute of Biotechnology, Nantong, China). Following incubation overnight at 4°C, horseradish peroxidase-conjugated goat anti-rabbit secondary antibody (1:2,000; cat. no. A0216; Beyotime Institute of Biotechnology) was added and incubated at room temperature for 2 h. Specific bands were visualized with an enhanced chemiluminescence reagent (KeyGen Biotech Co., Ltd.) on an autoradiographic film. For quantitative assay, images were analyzed using ImageJ software (version 1.48u; National Institutes of Health, Bethesda, MD, USA).

Animal studies. All animal studies were approved by the Animal Care and Welfare Committee of the Weifang People's Hospital and conducted in strict accordance with the guidelines of the National Animal Welfare Law of China. Female BALB/c nude mice (4-week-old; n=36; female; weight range, 20-25 g) were purchased from the Laboratory Animal Center of Yangzhou University (Yangzhou, China) and maintained in a specific-pathogen-free environment with a constant humidity (45-50%) and a constant temperature (25-27°C) under a 12 h light/dark cycle with *ad libitum* access to food and water. All mice were acclimatized for 1 week prior to the experiments. In order to identify the function of BRD4 *in vivo*, the mice (n=6/group) were subcutaneously injected into the right flanks with 2×10^6 shControl or shBRD4 SW1736 cells. A total of 3 weeks later, the mice were euthanized with the dislocation of cervical vertebra. In order to identify the association between BRD4 and GA *in vivo*, the mice were subcutaneously injected with 2×10^6 SW1736 cells transfected

with BRD4 plasmid (n=12/group) and control plasmid (n=12/group). Following injection, the mice were divided into 4 groups (n=6/group) (BRD4 plasmid group injected with BRD4 plasmid + 4 mg/kg GA; control plasmid group injected with control plasmid + 4 mg/kg GA) and immediately received GA treatment or 0.9% saline solution. The intravenous treatments were performed once every 3 days for a total of 21 days. The tumor volume (mm^3) was calculated using the following formula: Volume = $0.5 \times \text{length} \times \text{width}^2$. After 3 weeks, the mice were euthanized, and the tumors were isolated, weighed, photographed and analyzed by immunohistochemistry.

Immunohistochemistry. Paraffin-embedded archival specimens were cut into sections 4- μ m thick and baked at 65°C for 30 min. Sections were then dewaxed in xylene and rehydrated via graded alcohol solutions (100% ethanol, 5 min; 95% ethanol, 5 min; 70% ethanol, 5 min;), blocked in methanol containing 3% hydrogen peroxide for 10 min at room temperature, and then incubated with an BRD4 antibody (1:200; cat. no. ab75898; Abcam) anti-Ki67 antibody (1:200; cat. no. sc-23900; Santa Cruz Biotechnology, Inc.) at 4°C overnight. Following rinsing with PBS solution, biotinylated goat anti-rabbit serum IgG (1:2,000; cat. no. ab64256; Abcam) was used as a secondary antibody for 1 h at room temperature and the streptavidin peroxidase complex reagent was applied for 1 h at room temperature. Finally, the sections were incubated in a 3,3'-diaminobenzidine solution (DAB kit; Beyotime Institute of Biotechnology) at room temperature for 10 min and then counterstained with hematoxylin for 3 min at room temperature. Ten randomly selected visual fields per section were examined under a light microscope (magnification, x200) to evaluate the BRD4 and Ki67 expression.

Statistical analysis. Data are expressed as the mean \pm standard error. Statistical analysis was performed using SPSS version 13.0 software (SPSS, Inc., Chicago, IL, USA). Statistical significance was determined through unpaired Student's t-test or one-way analysis of variance. $P < 0.05$ was considered as an indicator of a statistically significant difference.

Results

Function of GA on the viability, proliferation and apoptosis of ATC cells. To illustrate the function of GA on ATC cell viability, a CCK-8 assay was conducted. SW1736 and KAT-18 cells were cultured with increasing doses of GA (0, 2, 4 and 6 μ g/ml) for 48 h. As shown in Fig. 1A, GA therapy for 48 h significantly inhibited the ATC cell viability in a dose-dependent manner. A CCK-8 assay was also performed on SW1736 and KAT-18 cells treated with 2 μ g/ml GA for the indicated time points (0, 24, 48 and 72 h). The results demonstrated that GA treatment decreased the viability of the two ATC cell lines in a time-dependent manner (Fig. 1B).

In order to investigate the function of GA on ATC cell proliferation, a colony formation assay was then performed. As shown in Fig. 1C, treatment of ATC cells with GA at different concentrations for 7 days significantly decreased the number of colonies in the cultures. The function of GA on ATC cell apoptosis was also examined by flow cytometry, and the results revealed that treatment of SW1736 and KAT-18

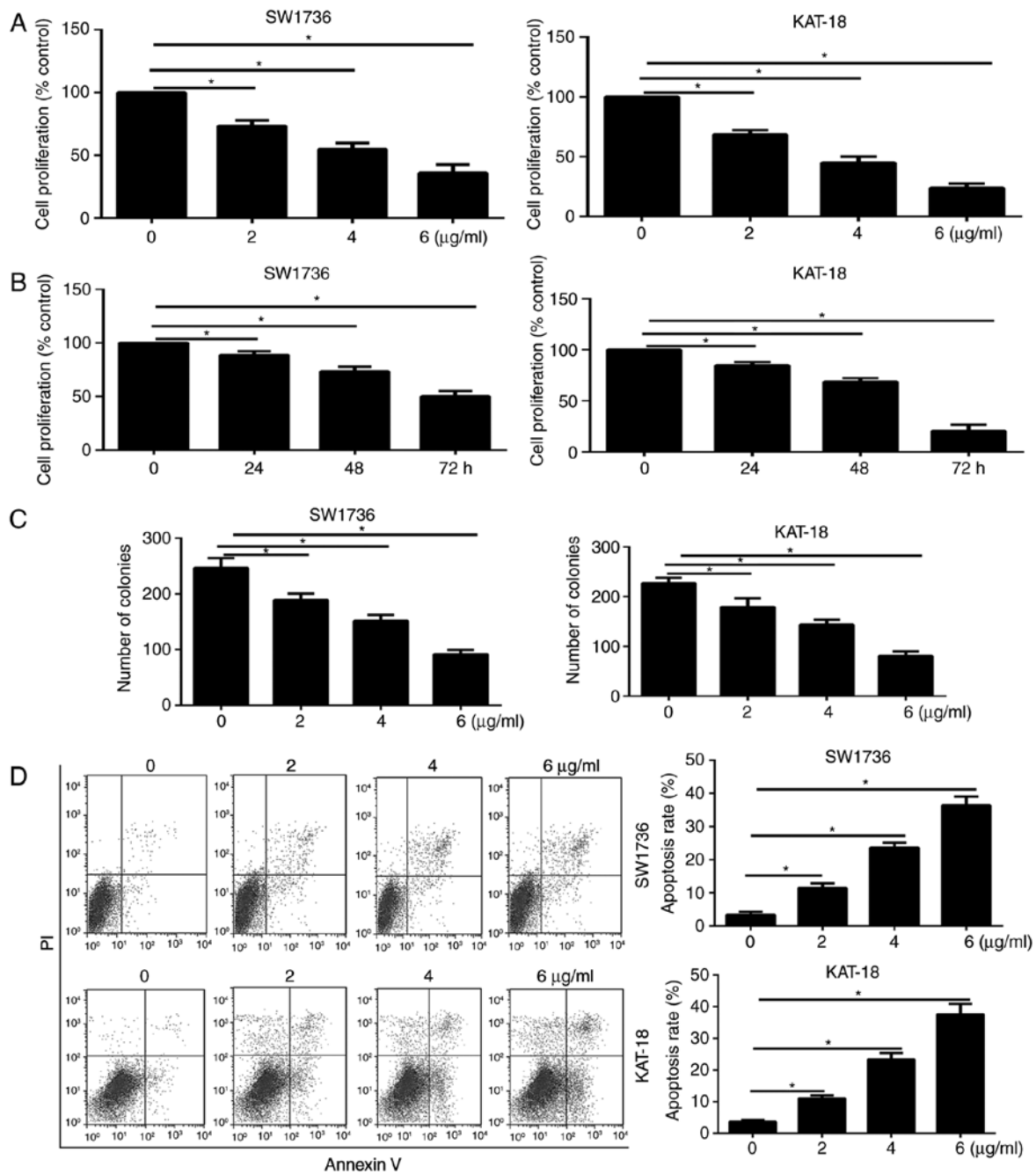


Figure 1. Effect of GA on the viability, proliferation and apoptosis of ATC cells. (A) SW1736 and KAT-18 cells were treated with (A) DMSO or GA (2, 4 and 6 $\mu\text{g/ml}$) for 48 h, and (B) 2 $\mu\text{g/ml}$ GA for 0, 24, 48 and 72 h. Following incubation, a cell counting kit-8 assay was performed to determine cell viability. The relative cell viability was defined as the percentage of cells treated with GA compared with the DMSO. (C) GA inhibited the colony formation of ATC cells treated with increasing doses of GA (0, 2, 4 and 6 $\mu\text{g/ml}$) for 7 days and then stained with crystal violet. (D) GA increased the apoptosis rate of ATC cells treated with increasing doses of GA (0, 2, 4 and 6 $\mu\text{g/ml}$) for 48 h. Cell apoptosis was evaluated by Annexin V-FITC/propidium iodide staining, followed by flow cytometric analysis. * $P < 0.05$ vs. corresponding control group. GA, gambogic acid; ATC, anaplastic thyroid cancer; DMSO, dimethyl sulfoxide; OD, optical density.

cells with GA for 48 h significantly enhanced the apoptosis rate (Fig. 1D) in a dose-dependent manner.

Expression of BRD4 is decreased by GA treatment in ATC cells. Previous studies have demonstrated that BRD4 served as an oncogene in papillary thyroid cancer (24,25). In the present study, we attempted to illustrate the association of GA and BRD4. The western blot assay demonstrated that GA treatment (2, 4 and 6 $\mu\text{g/ml}$) evidently decreased the protein expression

of BRD4 in SW1736 (Fig. 2A) and KAT-18 (Fig. 2B) cells. Furthermore, the RT-qPCR assay illustrated that GA treatment significantly decreased the mRNA expression of BRD4 in the two cell lines in a dose-dependent manner (Fig. 2C and D). Therefore, BRD4 may serve a critical role in the antitumor effect of GA in ATC.

Increased BRD4 expression in ATC tissues and cells. To determine the expression profile of BRD4 in ATC tissues,

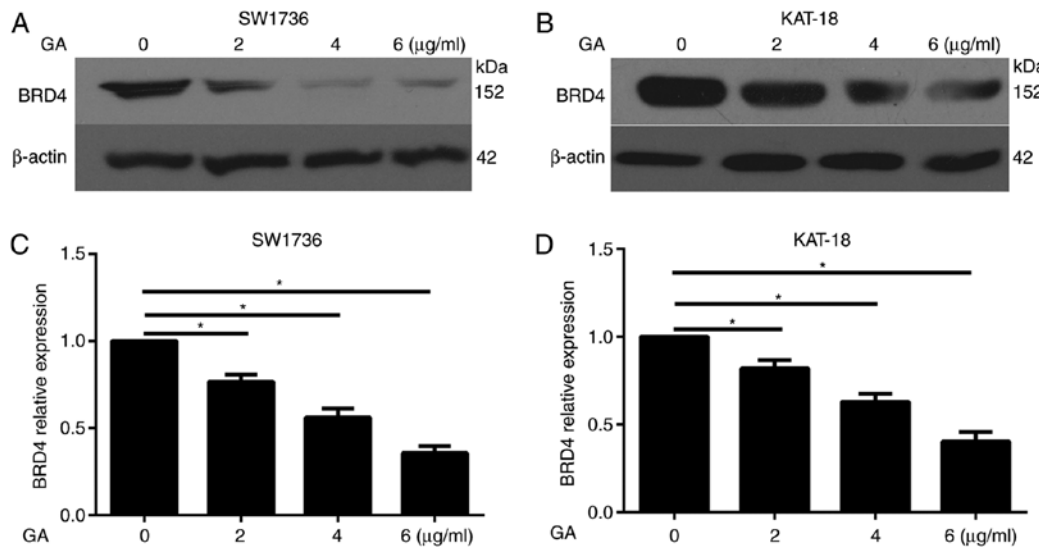


Figure 2. Effect of GA on BRD4 expression. Anaplastic thyroid cancer cells were exposed to increasing doses of GA (0, 2, 4 and 6 $\mu\text{g/ml}$) for 48 h. Subsequently, the protein expression of BRD4 was assayed by western blot analysis in (A) SW1736 and (B) KAT-18 cells, while the mRNA expression of BRD4 was examined by reverse transcription-quantitative polymerase chain reaction in (C) SW1736 and (D) KAT-18 cells. * $P < 0.05$. GA, gambogic acid; BRD4, bromodomain-containing protein 4.

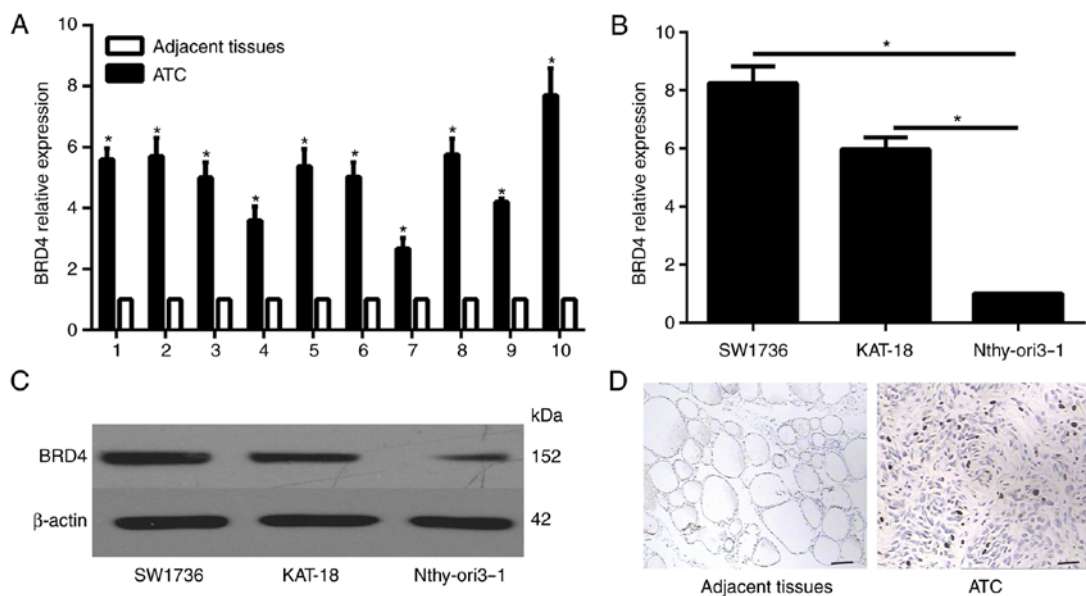


Figure 3. BRD4 is markedly upregulated in ATC tissues and cells. (A) RT-qPCR analysis of BRD4 mRNA expression in human ATC specimens and their corresponding normal thyroid tissues (n=10 pairs). (B) RT-qPCR and (C) western blot analysis were also used to examine the expression levels of BRD4 mRNA and protein, respectively, in human ATC cell lines SW1736 and KAT-18, and the human normal thyroid cell line Nthy-ori 3-1 (serving as a control). (D) Immunohistochemical staining of BRD4 in ATC specimens and their adjacent normal thyroid tissues (n=10 pairs) (magnification, $\times 200$). Scale bar=50 μm . * $P < 0.05$. ATC, anaplastic thyroid cancer; BRD4, bromodomain-containing protein 4; RT-qPCR, reverse transcription-quantitative polymerase chain reaction.

RT-qPCR was performed in 10 ATC specimens and their corresponding non-neoplastic thyroid tissues. Compared with the non-neoplastic thyroid tissues, the expression level of BRD4 was significantly enhanced in the ATC specimens (Fig. 3A). Furthermore, the mRNA and protein expression levels in normal thyroid and ATC cells were examined by RT-qPCR and western blot analysis, respectively. The results revealed that the mRNA and protein expression levels of BRD4 were significantly lower in the human thyroid Nthy-ori 3-1 cell line in comparison with those in the ATC cell lines (Fig. 3B and C). In addition, immunohistochemical analysis was conducted in

the patient specimens, and the results indicated that BRD4 was evidently overexpressed in ATC tissues as compared with that in the adjacent normal tissues (Fig. 3D).

BRD4 enhances the viability and proliferation of ATC cells in vitro. BRD4 was silenced in the SW1736 and KAT-18 cells in order to analyze the influence of this protein on the biological behavior of ATC cells. Western blot analysis was used to determine the expression level of BRD4, demonstrating that the shRNA transfection successfully downregulated BRD4 in the cells (Fig. 4A and B). Subsequently, the viability of the

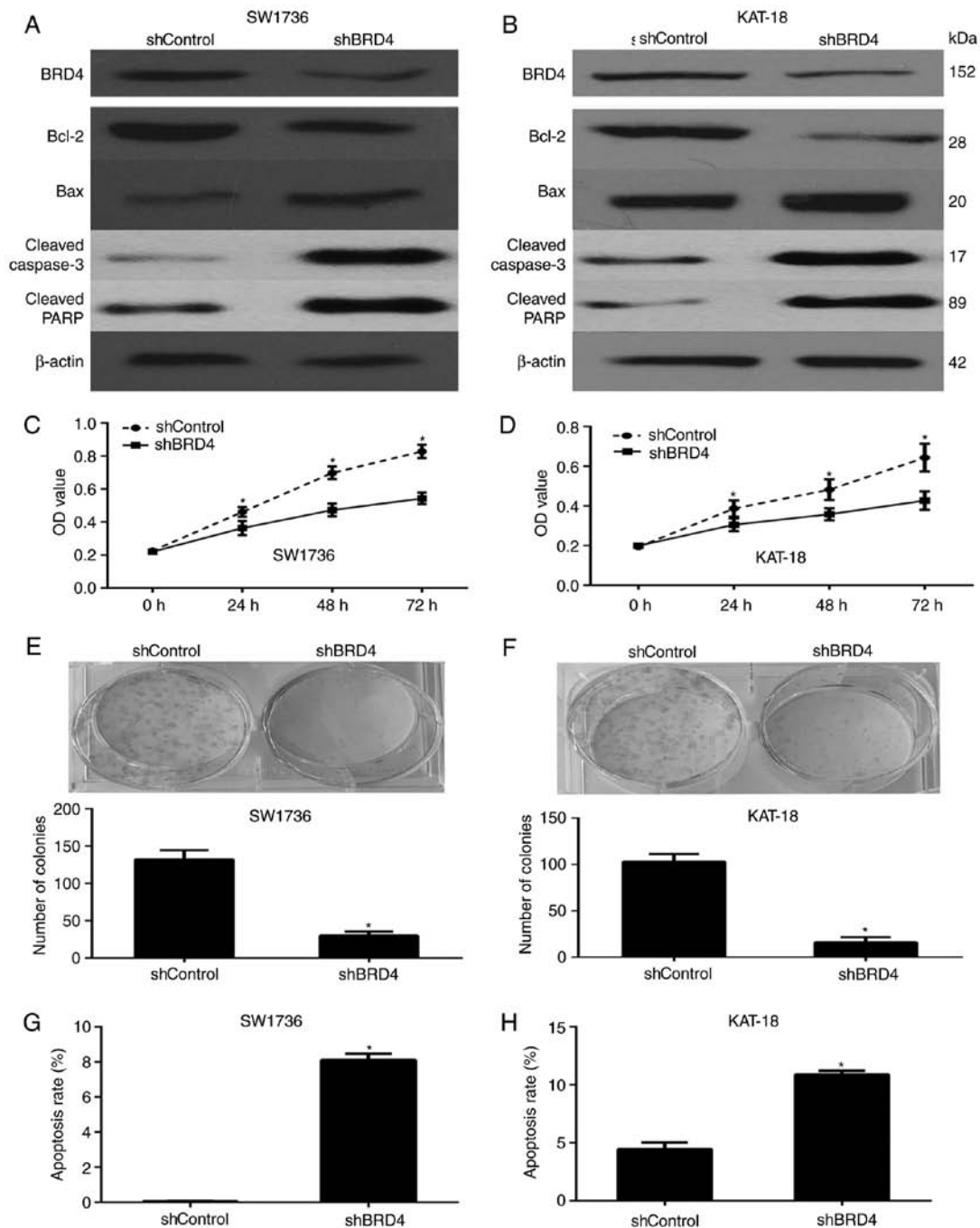


Figure 4. BRD4 expression enhances the proliferation and decreases the apoptosis in ATC cells. Protein expression levels of BRD4, Bcl-2, Bax, cleaved caspase-3 and cleaved PARP in the shControl- or shBRD4-transfected (A) SW1736 and (B) KAT-18 cells was determined via western blot analysis. The cell viability of (C) SW1736 and (D) KAT-18 cells was examined via a cell counting kit-8 assay, demonstrating that BRD4 silencing significantly inhibited ATC cell viability. BRD4 silencing in (E) SW1736 and (F) KAT-18 cells reduced the colony-forming efficiency. Annexin V-FITC/propidium iodide staining in (G) SW1736 and (H) KAT-18 cells transfected with shBRD4 demonstrated a higher apoptosis rate, as assessed via flow cytometry. * $P < 0.05$. BRD4, bromodomain-containing protein 4; Bcl-2, B-cell lymphoma 2; Bax, Bcl-2-associated X protein; PARP, poly(ADP-ribose) polymerase; ATC, anaplastic thyroid cancer.

SW1736 and KAT-18 cells was analyzed via a CCK-8 assay, and BRD4 silencing was observed to significantly decrease the viability of these cell lines (Fig. 4C and D). Furthermore, the colony formation assay demonstrated that the BRD4 knockdown significantly inhibited the proliferation of ATC cells (Fig. 4E and F), while the rate of apoptosis in these cells was markedly enhanced (Fig. 4G and H). All these data revealed that BRD4 is involved in the growth of ATC cells.

Western blotting was also performed to analyze the expression of apoptosis-associated proteins. In accordance with the

forementioned functional experiments, BRD4 silencing significantly decreased the expression of the anti-apoptotic factor Bcl-2, while it enhanced the expression levels of the pro-apoptotic factor Bax, cleaved caspase-3 and cleaved PARP in the SW1736 and KAT-18 cell lines (Fig. 4A and B).

BRD4 is essential for anaplastic thyroid cancer progression in vivo. To investigate the correlation of BRD4 expression with the ATC progression *in vivo*, SW1736 cells transfected with shBRD4 and shControl were subcutaneously injected

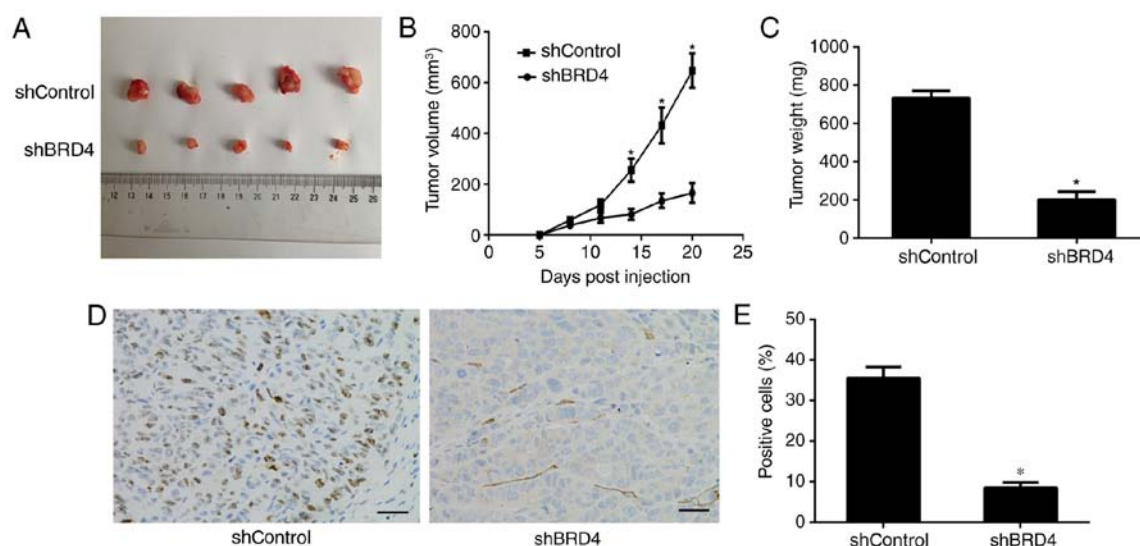


Figure 5. BRD4 maintains the tumorigenic capacity of anaplastic thyroid cancer *in vivo*. SW1736 cells transfected shControl or shBRD4 were injected subcutaneously into nude mice (n=6/group). At 3 weeks after cell implantation, the mice were sacrificed, tumor removed and photographed (A). In addition, the tumor volume (B) and weight (C) were measured. (D and E) Histologic analysis of tumor proliferation showed that shBRD4 tumors had significantly fewer Ki-67 positive cells. Scale bar=50 μ m. *P<0.05. BRD4, bromodomain-containing protein 4.

into nude mice (n=6/group). At 3 weeks after injection, the tumors were removed, and images were captured (Fig. 5A). The tumor volume and weight of the excised tumors indicated that BRD4 knockdown significantly delayed the tumor growth (Fig. 5B and C). Histological analysis of tumor proliferation also demonstrated that shBRD4 tumors had significantly fewer Ki-67 positive cells compared with those in the shControl tumors (Fig. 5D and E). These data illustrated that BRD4 expression enhanced ATC growth *in vivo*.

BRD4 is critical for the anti-cell growth effects of GA on ATC cells *in vitro*. To further illustrate the correlation of GA and BRD4, BRD4 expression was overexpressed by transfection with BRD4 overexpression plasmids. As shown in Fig. 6A and B, the BRD4 overexpression plasmid notably increased the expression of this protein in ATC cells compared with the control vector group.

ATC cells were then divided into four groups, treated with BRD4 overexpression plasmid + DMSO, BRD4 overexpression plasmid + 2 μ g/ml GA, control vector + DMSO, and control vector + 2 μ g/ml GA. The CCK-8 (Fig. 6C and D) and colony formation (Fig. 6E and F) assays revealed that overexpression of BRD4 was able to partially abrogate the inhibitory effects of GA on ATC cells. Furthermore, overexpression of BRD4 partially counteracted the suppression of cell apoptosis (Fig. 6G and H). Furthermore, the western blot analysis results demonstrated that BRD4 overexpression rescued the expression of the antiapoptotic protein Bcl-2, and counteracted the expression of pro-apoptosis gene Bax, which was induced by GA (Fig. 6A and B). Overexpression of BRD4 was demonstrated to counteract the effect of GA, so BRD4 down-regulation is critical for the antitumor growth effects of GA. These data manifested that GA inhibited the PTC progression through the inhibition of BRD4.

GA suppresses tumor growth through the inhibition of BRD4 *in vivo*. Tumor xenografts of SW1736 cells transfected with

BRD4 overexpression and control vector were used to evaluate the antitumor effect of GA (4 mg/kg) in nude mice *in vivo*. At 21 days after injection, the tumors were removed and images are shown in Fig. 7A. The periodic measurements of the tumor volume (Fig. 7B) and the final weight (Fig. 7C) of the excised tumors demonstrated that BRD4 overexpression was able to significantly abrogate the antitumor effects of GA on ATC cells.

Discussion

In vitro and *in vivo* studies have demonstrated that GA exerts potent antitumor effects on solid tumors and hematological malignancies, while may also induce apoptosis in other types of cancer cells (4-10). GA has been reported to promote apoptosis and resistance to metastatic potential in triple negative breast cancer (5). Furthermore, GA may enhance the efficiency of other chemical drugs in drug resistance tumour types via different molecular mechanisms. Gambogic acid sensitized resistant breast cancer cells to doxorubicin through inhibiting P-glycoprotein and suppressing survivin expression (7). GA as a non-competitive inhibitor of ATP-binding cassette transporter B1 reversed the multidrug resistance of human epithelial cancer types by promoting ATP-binding cassette transporter B1 protein degradation (8). GA sensitized ovarian cancer cells to doxorubicin through reactive oxygen species-mediated apoptosis (9). A combination of GA with cisplatin enhanced the antitumor effects on cisplatin-resistant lung cancer cells by downregulating multidrug resistance-associated protein 2 and low density lipoprotein receptors expression (10). In the present study, it was observed that BRD4 expression was decreased by GA treatment. Furthermore, BRD4 silencing enhanced the apoptosis rate and decreased the proliferation of ATC cell lines.

Consistent with previous findings (5), the current study results confirmed that GA treatment significantly decreased the viability and proliferation of SW1736 and KAT-18 cells

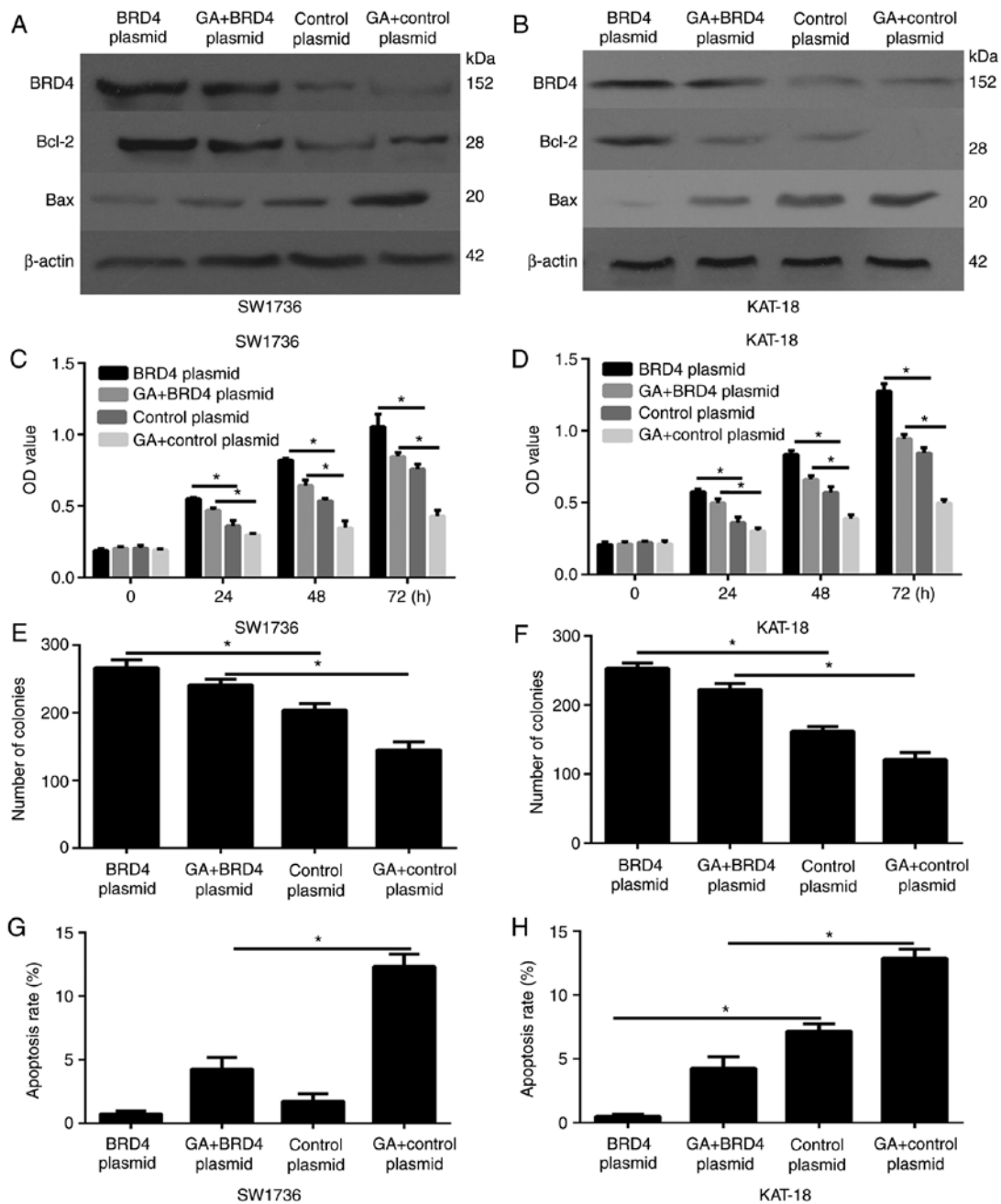


Figure 6. BRD4 is critical for the anti-cell growth effects of GA on ATC cells. SW1736 and KAT-18 cells transfected with BRD4 overexpression plasmid or control vector, were treated with 2 μ g/ml for 48 h, the protein expression of BRD4, Bcl-2 and Bax was determined using western blotting (A and B). (C and D) Cell viability was determined via CCK-8 assay at indicated time points. (E and F) Colony formation assay showed that BRD4 overexpression significantly rescue the inhibitory effects of GA on ATC cells. (G and H) Overexpression of BRD4 could partially counteract the suppressing cell apoptosis. * P <0.05. GA, gambogic acid; ATC, anaplastic thyroid cancer; BRD4, bromodomain-containing protein 4.

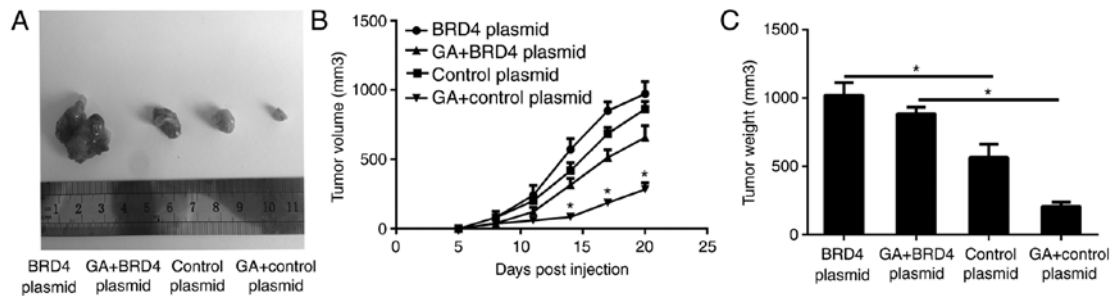


Figure 7. GA suppresses tumor growth through the inhibition of BRD4 *in vivo*. BRD4 overexpression and control vector SW1736 cells were injected subcutaneously into BALB/c nude mice (n=6/group) and treated with GA (4 mg/kg) for 21 days. The mice were sacrificed, tumor removed and photographed (A). In addition, the tumor size (B) and weight (C) were measured. * P <0.05. GA, gambogic acid; BRD4, bromodomain-containing protein 4.

by increasing the cell apoptosis rate (Fig. 1). Western blot analysis and RT-qPCR results also revealed that the expression level of BRD4 was significantly decreased following GA treatment (Fig. 2). Furthermore, BRD4 was significantly upregulated in ATC tissues as compared with that in normal thyroid tissues (Fig. 3). These data suggested that BRD4 may be involved in ATC pathogenesis and may serve as a target for GA.

The epigenetic mechanism is a rapidly progressing field in oncological research, and the modulation of epigenetic regulators is considered as an alternative therapeutic strategy for cancer (13). BRD4 is a member of the BET family of proteins, which contain two bromodomains in tandem and an extra-terminal domain (13,14). It has been reported that BRD4, as a conserved epigenome regulator, regulates the expression of numerous genes involved in cell growth, cell cycle progression and inflammation in different types of cancer (13,14). The inhibition of BRD4 in papillary thyroid cancer cells by JQ1 has been demonstrated to result in cell cycle arrest at G₀/G₁ phase, enhance ¹³¹I uptake *in vitro* and suppress tumor growth *in vivo*. JQ1 is also able to inhibit the proliferation of ATC *in vitro* (24,25). However, the function of BRD4 in ATC has yet to be fully clarified.

In the present study, silencing BRD4 in ATC cells was observed to repress their viability, proliferation and apoptosis (Fig. 4), whereas BRD4 overexpression caused the opposite effects on these cells (Fig. 6). Furthermore, *in vivo* results demonstrated that BRD4 was involved in tumor growth (Figs. 5 and 7) and thus may serve as an antitumor target in ATC. Furthermore, the current study aimed to explore the molecular mechanism by which BRD4 functions as an oncogene in ATC. The results revealed that BRD4 silencing was associated with the downregulation of the anti-apoptotic protein Bcl-2 and the upregulation of the pro-apoptotic protein Bax. These data indicated that BRD4 promoted tumor growth by inhibiting cell apoptosis.

In order to further investigate the association between GA and BRD4, BRD4 expression was upregulated through transfection with a BRD4 overexpression plasmid in SW1736 and KAT-18 cells. The biological effects of GA on ATC cells were significantly weakened by BRD4 overexpression (Fig. 6), suggesting that GA partially exerted its anticancer functions by downregulating BRD4. The apoptosis rate of ATC cells was significantly decreased by GA and partially rescued by BRD4 overexpression. These results demonstrated that GA regulated BRD4 and induced apoptosis.

In conclusion, the results of the present study suggested that BRD4 serves an important role in ATC progression *in vitro* and *in vivo*, and may function as a novel target for the development of alternative therapeutic approaches for cancer. Furthermore, BRD4 is essential for the antiproliferative and pro-apoptotic effects of GA on ATC.

Acknowledgements

Not applicable.

Funding

The current study was supported by the Foundation of Shandong People and Family Planning Commission (grant no. 2015WSA07008).

Availability of data and materials

All data generated or analyzed during this study are included in this published article.

Authors' contributions

HS conceived and designed the experiments. WW wrote and revised the manuscript. YW conducted all experiments. All authors read and approved the final manuscript.

Ethics approval and consent to participate

The present study was approved by the ethics committee of Weifang People's Hospital (Weifang, China). All patients provided written informed consent for the publication of any associated data and accompanying images.

Consent for publication

Not applicable.

Competing interests

The authors declare that they have no competing interests.

References

1. Siegel RL, Miller KD and Jemal A: Cancer statistics, 2017. *CA Cancer J Clin* 67: 7-30, 2017.
2. Nagaiah G, Hossain A, Mooney CJ, Parmentier J and Remick SC: Anaplastic thyroid cancer: A review of epidemiology, pathogenesis, and treatment. *J Oncol* 2011: 542358, 2011.
3. O'Neill JP and Shaha AR: Anaplastic thyroid cancer. *Oral Oncol* 49: 702-706, 2013.
4. Qi Q, Lu N, Wang XT, Gu HY, Yang Y, Liu W, Li C, You QD and Guo QL: Anti-invasive effect of gambogic acid in MDA-MB-231 human breast carcinoma cells. *Biochem Cell Biol* 86: 386-395, 2008.
5. Li C, Qi Q, Lu N, Dai Q, Li F, Wang X, You Q and Guo Q: Gambogic acid promotes apoptosis and resistance to metastatic potential in MDA-MB-231 human breast carcinoma cells. *Biochem Cell Biol* 90: 718-730, 2012.
6. Li D, Song XY, Yue QX, Cui YJ, Liu M, Feng LX, Wu WY, Jiang BH, Yang M, Qu XB, *et al*: Proteomic and bioinformatic analyses of possible target-related proteins of gambogic acid in human breast carcinoma MDA-MB-231 cells. *Chin J Nat Med* 13: 41-51, 2015.
7. Wang S, Wang L, Chen M and Wang Y: Gambogic acid sensitizes resistant breast cancer cells to doxorubicin through inhibiting P-glycoprotein and suppressing survivin expression. *Chem Biol Interact* 235: 76-84, 2015.
8. Wang X, Deng R, Lu Y, Xu Q, Yan M, Ye D and Chen W: Gambogic acid as a non-competitive inhibitor of ATP-binding cassette transporter B1 reverses the multidrug resistance of human epithelial cancers by promoting ATP-binding cassette transporter B1 protein degradation. *Basic Clin Pharmacol Toxicol* 112: 25-33, 2013.
9. Wang J and Yuan Z: Gambogic acid sensitizes ovarian cancer cells to doxorubicin through ROS-mediated apoptosis. *Cell Biochem Biophys* 67: 199-206, 2013.
10. Zhang W, Zhou H, Yu Y, Li J, Li H, Jiang D, Chen Z, Yang D, Xu Z and Yu Z: Combination of gambogic acid with cisplatin enhances the antitumor effects on cisplatin-resistant lung cancer cells by downregulating MRP2 and LRP expression. *Oncotargets Ther* 9: 3359-3368, 2016.
11. Liu WY, Wu XU, Liao CQ, Shen J and Li J: Apoptotic effect of gambogic acid in esophageal squamous cell carcinoma cells via suppression of the NF- κ B pathway. *Oncol Lett* 11: 3681-3685, 2016.

12. Yang Z, He N and Zhou Q: Brd4 recruits P-TEFb to chromosomes at late mitosis to promote G₁ gene expression and cell cycle progression. *Mol Cell Biol* 28: 967-976, 2008.
13. Wang YH, Sui YN, Yan K, Wang LS, Wang F and Zhou JH: BRD4 promotes pancreatic ductal adenocarcinoma cell proliferation and enhances gemcitabine resistance. *Oncol Rep* 33: 1699-1706, 2015.
14. Wang YH, Sui XM, Sui YN, Zhu QW, Yan K, Wang LS, Wang F and Zhou JH: BRD4 induces cell migration and invasion in HCC cells through MMP-2 and MMP-9 activation mediated by the Sonic hedgehog signaling pathway. *Oncol Lett* 10: 2227-2232, 2015.
15. Segura MF, Fontanals-Cirera B, Gazieli-Sovran A, Guijarro MV, Hanniford D, Zhang G, González-Gomez P, Morante M, Jubierre L, Zhang W, *et al*: BRD4 sustains melanoma proliferation and represents a new target for epigenetic therapy. *Cancer Res* 73: 6264-6276, 2013.
16. Puissant A, Frumm SM, Alexe G, Bassil CF, Qi J, Chanthery YH, Nekritz EA, Zeid R, Gustafson WC, Greninger P, *et al*: Targeting MYCN in neuroblastoma by BET bromodomain inhibition. *Cancer Discov* 3: 308-323, 2013.
17. Cheng Z, Gong Y, Ma Y, Lu K, Lu X, Pierce LA, Thompson RC, Muller S, Knapp S and Wang J: Inhibition of BET bromodomain targets genetically diverse glioblastoma. *Clin Cancer Res* 19: 1748-1759, 2013.
18. Patel AJ, Liao CP, Chen Z, Liu C, Wang Y and Le LQ: BET bromodomain inhibition triggers apoptosis of NF1-associated malignant peripheral nerve sheath tumors through Bim induction. *Cell Rep* 6: 81-92, 2014.
19. Ott CJ, Kopp N, Bird L, Paranal RM, Qi J, Bowman T, Rodig SJ, Kung AL, Bradner JE and Weinstock DM: BET bromodomain inhibition targets both c-Myc and IL7R in high-risk acute lymphoblastic leukemia. *Blood* 120: 2843-2852, 2012.
20. Lockwood WW, Zejnullahu K, Bradner JE and Varmus H: Sensitivity of human lung adenocarcinoma cell lines to targeted inhibition of BET epigenetic signaling proteins. *Proc Natl Acad Sci USA* 109: 19408-19413, 2012.
21. Andrieu G, Tran AH, Strissel KJ and Denis GV: BRD4 regulates breast cancer dissemination through Jagged1/Notch1 signaling. *Cancer Res* 76: 6555-6567, 2016.
22. Molinaro E, Romei C, Biagini A, Sabini E, Agate L, Mazzeo S, Materazzi G, Sellari-Franceschini S, Ribechini A, Torregrossa L, *et al*: Anaplastic thyroid carcinoma: From clinicopathology to genetics and advanced therapies. *Nat Rev Endocrinol* 13: 644-660, 2017.
23. Livak KJ and Schmittgen TD: Analysis of relative gene expression data using real-time quantitative PCR and the 2^{-ΔΔCT} method. *Methods* 25: 402-408, 2001.
24. Gao X, Wu X, Zhang X, Hua W, Zhang Y, Maimaiti Y, Gao Z and Zhang Y: Inhibition of BRD4 suppresses tumor growth and enhances iodine uptake in thyroid cancer. *Biochem Biophys Res Commun* 469: 679-685, 2016.
25. Mio C, Lavarone E, Conzatti K, Baldan F, Toffoletto B, Puppini C, Filetti S, Durante C, Russo D, Orlacchio A, *et al*: MCM5 as a target of BET inhibitors in thyroid cancer cells. *Endocr Relat Cancer* 23: 335-347, 2016.



This work is licensed under a Creative Commons Attribution-NonCommercial-NoDerivatives 4.0 International (CC BY-NC-ND 4.0) License.